Original Article

Estimation of hypoperfused tissue volume in large vessel occlusions: pseudo-continuous arterial spin labeling versus dynamic susceptibility contrast perfusion-weighted imaging

Chenxi Zhao[1#], Chen Cao[2#], Lei Ren[3,4#], Huiying Wang[5], Gemuer Wu[6], Dingwei Fu[1], Jinxia Zhu[7], Chao Chai[5], Yu Guo[5], Shuang Xia[5]

[1]Department of Radiology, The First Central Clinical School, Tianjin Medical University, Tianjin, China; [2]Department of Radiology, Tianjin Huanhu Hospital, Tianjin, China; [3]Medical Imaging Department, First Teaching Hospital of Tianjin University of Traditional Chinese Medicine, Tianjin, China; [4]National Clinical Research Center for Chinese Medicine Acupuncture and Moxibustion, Tianjin, China; [5]Department of Radiology, Medical Imaging Institute of Tianjin, Tianjin First Central Hospital, School of Medicine, Nankai University, Tianjin, China; [6]Department of Radiology, Affiliated Hospital of Inner Mongolia Medical University, Hohhot, China; [7]MR Collaboration, Siemens Healthineers Ltd., Beijing, China

Contributions: (I) Conception and design: C Zhao, C Cao, L Ren; (II) Administrative support: C Zhao, C Cao, L Ren, J Zhu; (III) Provision of study materials or patients: C Zhao, C Cao, L Ren, H Wang, D Fu; (IV) Collection and assembly of data: C Zhao, C Cao, L Ren, G Wu, C Chai; (V) Data analysis and interpretation: C Zhao, C Cao, L Ren, Y Guo, S Xia; (VI) Manuscript writing: All authors; (VII) Final approval of manuscript: All authors.

[#]These authors contributed equally to this work as co-first authors.

Correspondence to: Shuang Xia, MD; Yu Guo, MD. Department of Radiology, Medical Imaging Institute of Tianjin, Tianjin First Central Hospital, School of Medicine, Nankai University, No. 2 Baoshan West Road, Xiqing District, Tianjin 300192, China. Email: xiashuang77@163.com; yummy8106@163.com.

Background: Currently, the selection of patients with acute anterior large vessel occlusions (LVOs) for endovascular thrombectomy (EVT) is primarily based on dynamic susceptibility contrast perfusion-weighted imaging (DSC-PWI) or computed tomography (CT) perfusion imaging. This study investigated the consistency between hypoperfused tissue (HPT) (time to maximum >6 s, Tmax >6 s) volumes estimated by corrected and uncorrected multidelay pseudo-continuous arterial spin labeling (pCASL) and DSC-PWI in patients with anterior LVOs and also evaluated the diagnostic performances in selecting patients with acute LVOs for EVT.

Methods: This retrospective study enrolled patients with acute (n=108) and symptomatic chronic (n=90) LVOs. Shapiro-Wilk tests and receiver operating characteristic (ROC) analyses were used. Intraclass correlation coefficient (ICC) compared the consistency of HPT volume calculated by DSC-PWI and multidelay pCASL.

Results: Multidelay pCASL with different thresholds in acute LVOs were 128.8 [interquartile range (IQR), 76.2–181.1] mL in uncorrected relative cerebral blood flow (rCBF) <40%, 84.1 (IQR, 36.8–133.9) mL in uncorrected CBF <20 mL·100 g^{-1}·min^{-1}, and 74.4 (IQR, 26.2–118.0) mL in corrected CBF <20 mL·100 g^{-1}·min^{-1}, which were comparable to the volume of 69.5 (IQR, 20.0–121.4) mL automatically determined by Tmax >6 s in DSC-PWI, and showed substantial consistency after correction (ICC =0.742). Multidelay pCASL with different thresholds in symptomatic chronic LVOs was 78.3 (IQR, 53.5–129.4) mL, 59.8 (IQR, 16.6–98.5) mL and 36.4 (IQR, 10.1–85.3) mL, which were comparable to the volume of 0 (IQR, 0–36.4) mL in DSC-PWI, and showed substantial consistency after correction (ICC =0.617). Using DEFUSE 3 as the reference standard, the CBF corrected by arterial transit time (ATT) showed good performance in selecting patients for EVT (area under the curve 0.804, 95% confidence interval: 0.717–0.891).

Conclusions: The volume of HPT defined by corrected CBF <20 mL·100 g^{-1}·min^{-1} is consistent with that

of DSC-PWI in acute and chronic symptomatic LVOs patients. Multidelay pCASL adjusted by ATT is more applicable to clinical routine.

Keywords: Acute ischemic stroke (AIS); arterial spin labeling (ASL); large vessel occlusions (LVOs); hypoperfused tissue volume

Submitted Jul 31, 2024. Accepted for publication Jan 07, 2025. Published online Feb 26, 2025.
doi: 10.21037/qims-24-1560
View this article at: https://dx.doi.org/10.21037/qims-24-1560

Introduction

Stroke is a leading cause of mortality and long-term disability worldwide, with new stroke cases reaching approximately 3.94 million annually (1). In China, ischemic stroke accounted for nearly 81.9% of all the stroke-related cases; 20% of these cases were due to acute ischemic stroke (AIS) from anterior large vessel occlusions (LVOs) in 2019 (2). The DEFUSE-3 and DAWN trials demonstrated that endovascular thrombectomy (EVT) improved the benefit window between 6–24 hours for selected patients with LVOs in the anterior circulation (3,4). Perfusion imaging is generally used to select patients with AIS and salvageable ischemic brain tissue for EVT (5). AIS patients exhibiting specific patterns of penumbra tissue—which refers to the volume of brain tissue that is ischemic but has not yet progressed to infarction—may derive benefits from endovascular reperfusion therapy even beyond the conventional 6-hour window from the onset of symptoms. Penumbral volume, measured using automated software, has been defined as the volume of tissue with critical hypoperfusion tissue (HPT) (time to maximum >6 s, Tmax >6 s) minus the volume of the ischemic core (6). The analysis of cerebral hemodynamics in patients with symptomatic chronic occlusive disease is important for determining the clinical treatment strategy and prognosis (7). Computed tomography perfusion (CTP) imaging has shown that the incidence of border zone infarction and cognitive impairment is significantly higher in ischemic stroke patients with symptomatic chronic occlusions that demonstrate benign oligemia (8). Estimation of the hypoperfused area is critical in determining the clinical outcomes of stroke patients.

Arterial spin labeling (ASL) is a non-invasive magnetic resonance imaging (MRI) technique that can be used to estimate cerebral blood flow (CBF). Previous studies have shown that the ASL-CBF is comparable to the dynamic susceptibility contrast perfusion-weighted imaging (DSC-PWI) in delineating the HPT regions in patients with AIS (9,10). Recently, multidelay ASL has employed multiple post-labeling delays (PLDs) to achieve the optimal perfusion parameters, which yields more accurate CBF by correction of arterial transit time (ATT) instead of the assumption that ATT equals labeling delay time (11). ASL would be advantageous over DSC-PWI and CTP for patients with impaired renal function because it can estimate perfusion parameters without using radiation or contrast agents and can perform repetitive perfusion imaging (12,13). Furthermore, non-invasive quantification of the volume of the ischemic penumbra is essential for defining the treatment strategy for stroke patients with acute LVOs.

We hypothesized that a background-suppressed 3-dimensional (3D) pulse sequence in conjunction with a multi-delay pseudo-continuous ASL (pCASL) would accurately identify and estimate the volumes of HPT in patients with acute and symptomatic chronic anterior LVOs. Therefore, in this study, we compared the volumes of the HPT as estimated by the multidelay pCASL and the DSC-PWI techniques in patients with acute and symptomatic chronic anterior LVOs. We also evaluated the prediction performance of pCASL data to select patients with acute anterior LVOs for EVT. We present this article in accordance with the STROBE reporting checklist (available at https://qims.amegroups.com/article/view/10.21037/qims-24-1560/rc).

Methods

Patient selection

This retrospective study was conducted in accordance with the Declaration of Helsinki (as revised in 2013). The study was approved by institutional ethics board of Tianjin First Central Hospital (No. 2017N002KY) and the requirement of individual consent for this retrospective analysis was waived. This study included 368 patients with LVOs

of the anterior circulation based on the time of flight-magnetic resonance angiography (TOF-MRA) assessment between June 2018 and March 2021. These patients were simultaneously subjected to DSC-PWI, diffusion-weighted imaging (DWI), and multi-delay pCASL. The patient demographics and the characteristics of the ischemic strokes based on the DWI, apparent diffusion coefficient (ADC) values, and the T2-weighted imaging (T2WI) were evaluated.

The inclusion criteria for patients with acute LVOs were as follows: (I) AIS was observed within 6–24 hours of symptom onset; and (II) acute ischemic lesions were detected in the DWI. The exclusion criteria were as follows: (I) patient motion artifacts that affected the diagnosis; and (II) >50% stenosis on the MRA in the contralateral internal cerebral artery (ICA) or middle cerebral artery (MCA), which may affect brain perfusion.

The inclusion criteria for patients with symptomatic chronic LVOs were as follows: (I) duration of the occlusion was 4 weeks or more (14,15); (II) presence of recurrent ischemic neurological deficits including transient ischemic attacks or stroke; and (III) DWI showing border zone infarction and/or perfusion images showing Tmax >4 s. The exclusion criteria were as follows: (I) poor MR image quality of pCASL; (II) >50% stenosis in the contralateral large vessels of the anterior circulation; (III) non-atherosclerotic occlusions related to moyamoya disease or angiitis disease; and (IV) symptom aggravation due to hemorrhagic transformation of the infarction or new infarction in a non-occluded vessel.

MRI data acquisition

MRI was performed using a 3T MRI scanner (MAGNETOM Prisma; Siemens Healthcare, Erlangen, Germany) equipped with a 64-channel head-neck coil. pCASL and DWI data were acquired before injecting the contrast for DSC-PWI acquisitions. The standard MRI protocol for the stroke patients included axial T2WI, DWI, MRA, pCASL, and DSC brain perfusion imaging. The DWI data was acquired using a single-shot echo planar imaging (EPI) sequence with following parameters: time of repetition (TR) =2,900 ms; time of echo (TE) =73 ms; field of view (FOV) =240×240 mm^2, matrix =168×134; slice thickness =5 mm; number of slices =19; GeneRalized Autocalibrating Partial Parallel Acquisition (GRAPPA) acceleration factor =2; 2 b values (0 and 1,000 s/mm^2) were applied in 4 diffusion directions; acquisition time =23 s. The ASL scans were performed using a 5-delay pCASL pulse sequence and background suppressed 3-dimensional gradient and spin-echo readout with the following parameters: TR =4,600 ms; TE =32 ms; FOV =224×224 mm^2; matrix =64×64; slice thickness =3.5 mm; number of slices =32; labeling pulse duration =1.5 s; PLD =1/1.5/2/2.5/3 s; GRAPPA acceleration factor =2; acquisition time =6 min 3 s. The M0 scan was also acquired without labeling or suppression pulses. The reasons for the choice of 1/1.5/2/2.5/3 s for PLD are given in Appendix 1. The DSC-PWI was acquired using an EPI sequence with following parameters: TR =1,500 ms; TE =30 ms; FOV =220×220 mm^2, matrix =128×128; slice thickness =5 mm; number of slices = 19; GRAPPA acceleration factor =2; acquisition time =1 min 38 s. DSC-PWI was performed by administering 0.1 mmol/kg of the gadolinium-based contrast agent (Magnevist; Schering, Berlin, Germany) at a rate of 3 mL/s. DSC-PWI analysis was performed by acquiring 60 measurements for each section. The specific imaging parameters of the MRI sequences are listed in Table S1.

Postprocessing of MRI data and automated estimation of the hypoperfused lesions

The DWI and DSC-PWI data analyses were performed with automated RAPID software (iSchemaView; Menlo Park, CA, USA), and the volume of the ischemic core and penumbra regions were estimated. The ADC values based on the DWI were used to quantify the ischemic core. PWI required selection of a global arterial input function from an unaffected anterior cerebral artery and a venous outflow function from a large draining vein (sagittal sinus). Deconvolution of the tissue enhancement curve and the arterial input function was performed using model-free singular value decomposition. Tmax >6 s was used for calculating the total HPT in software, and penumbra and infarct volume was quantified within the whole scan range. The ischemic core was defined as ADC <620×10^{-6} mm^2/s. The penumbra was defined as the volume of tissue between Tmax >6 s and infarct core.

The postprocessing and analysis of the multi-delay pCASL data was performed using a commercial software by Anying Technology Beijing Co., Ltd. (aStroke, ischemic penumbra module of CereFlow automatic calculation software; Beijing, China). The ASL images were first subjected to motion correction. Then, pairwise subtraction was performed between the labeled and the control images

to generate the mean difference images for each PLD. An uncorrected CBF image was calculated according to formula with total signal intensity image. An ATT-corrected CBF image was calculated according to the following formula with total signal intensity image and ATT image (δ) (11,16):

$$cCBF = \frac{6000e^{\delta/T_{1a}}}{2\varepsilon T_{1a}\left(e^{-\max(PLD-\delta,0)/T_{1t}}-e^{-\max(LD+PLD-\delta,0)/T_{1t}}\right)}\frac{SI\cdot Sr}{M0} \quad [1]$$

where CBF reflects the cerebral blood flow in mL·100 g^{-1}·min^{-1}, δ is the arterial transit delay, PLD is the shortest post labeling delay (1.0 s), LD is the entire labeling duration (4.0 s), T_{1a} is the longitudinal relaxation of arterial blood (1.6 s), T_{1t} is the longitudinal relaxation of gray matter (1.2 s), is the combined efficiency of labeling and background suppression (0.6375), SI is the signal intensity in the PWI, and M0 is the signal intensity of the reference image. The reference image is scaled by Sr = λ (1 – $e^{-2/1.2}$) to account for the combined effect of the blood–brain partition coefficient (lambda 0.9) and the partial GM signal recovery in a 2-s saturation-recovery reference image.

The volume of the ischemic core was measured using the RAPID software. The uncorrected relative CBF (rCBF) values were defined as ipsilateral divided by the contralateral measurements. Hypoperfusion regions of uncorrected rCBF were obtained at 40%. This cut-off was based on a previous study, which demonstrated that the hypoperfused regions corresponding to 40% reduced CBF relative to the contralateral regions correlated with the penumbra (17). One region of absolute value of corrected CBF (cCBF) was obtained according to the range: 0 to 20 mL·100 g^{-1}·min^{-1}. The penumbra was defined as the volume of HPT minus the volume of infarct core.

All the source MR images and the estimates of the hypoperfused lesions from the DSC-PWI and multi-delay pCASL datasets were independently reviewed and validated by 2 experienced neuroradiologists with 10 years of experience. The neuroradiologists were not blinded to the software. The reports were evaluated in terms of correct placement of the arterial input function and misregistration of regions outside the territory of the occluded artery. The inclusion criteria were based on the DEFUSE-3 trial (3). Patients with an ischemic core of <70 mL, ratio of the ischemic tissue volume to the initial infarct volume ≥1.8, and a penumbra size of ≥15 mL were considered for thrombectomy.

Statistical analysis

Statistical analysis was performed using the software SPSS 23.0 (IBM Corp., Armonk, NY, USA) and GraphPad Prism 9.0 (GraphPad Software Inc., San Diego, CA, USA) software. Descriptive statistics were used to quantify the differences among the HPT volumes and penumbra calculated using the 2 techniques. The mean values were used for normally distributed data and median values were used for non-normally distributed data. The Shapiro-Wilk test was used to compare the normally distributed data. The estimated volumes and the ratios were not normally distributed because the occlusions of different vascular sections resulted in the hypoperfusion of multiple cerebral areas. Intraclass correlation coefficient (ICC) compared the consistency of HPT volume calculated by DSC-PWI and multidelay ASL. ICC 0.41–0.60 was moderate, 0.61–0.80 substantially consistent, and 0.81–1.00 almost perfect (excellent). The receiver operating characteristic (ROC) curve was performed to assess the prediction performance of pCASL data to select patients for mechanical thrombectomy. All tests were 2-sided with a significance level of 0.05.

Results

Basic characteristics of the participants

The patient selection strategy used in this study is shown in *Figure 1*. Initially, 368 consecutive patients with LVOs were enrolled in this study. Finally, 198 patients, comprising 108 (55%) with acute LVOs and 90 (45%) with symptomatic chronic LVOs, were included in the study. *Table 1* shows the clinical and imaging characteristics of the included patients with acute and symptomatic chronic LVOs.

Consistency of HPT volumes based on the corrected pCASL and the DSC-PWI in patients with acute and symptomatic chronic LVOs

Multidelay ASL with different thresholds in acute LVOs were 128.8 [interquartile range (IQR), 76.2–181.1] mL in uncorrected rCBF <40%, 84.1 (IQR, 36.8–133.9) mL in uncorrected CBF <20 mL·100 g^{-1}·min^{-1}, and 74.4 (IQR, 26.2–118.0) mL in cCBF <20 mL·100 g^{-1}·min^{-1}, which were compared with the volume of 69.5 (IQR, 20.0–121.4) mL automatically determined by Tmax >6 s in DSC-PWI. Multidelay ASL with different thresholds in symptomatic chronic LVOs were 78.3 (IQR, 53.5–129.4) mL in uncorrected rCBF <40%, 59.8 (IQR, 16.6–98.5) mL in uncorrected CBF <20 mL·100 g^{-1}·min^{-1}, and 36.4 (IQR,

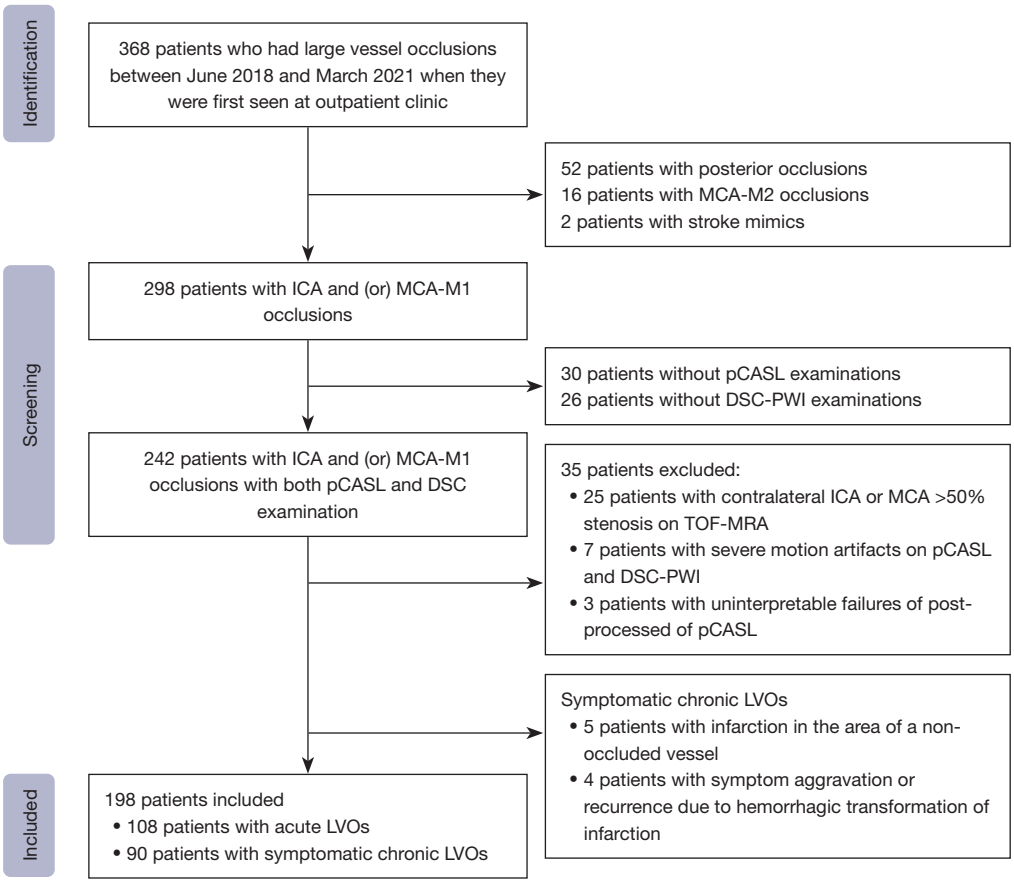

Figure 1 Flowchart of the patient selection strategy. ICA, internal carotid artery; MCA-M1, first segment of the middle cerebral artery; MCA-M2, second segment of the middle cerebral artery; pCASL, pseudo-continuous arterial spin labeling; DSC-PWI, dynamic susceptibility contrast perfusion weighted imaging; LVOs, large vessel occlusions; TOF-MRA, time of flight-magnetic resonance angiography.

10.1–85.3) mL in cCBF <20 mL·100 g^{-1}·min^{-1}, which were compared with the volume of 0 (IQR, 0–36.4) mL automatically determined by Tmax >6 s in DSC-PWI. The specific change in hypoperfusion volume before and after corrected by ATT are provided in *Figure 2*.

In the acute group, hypoperfusion volume defined by uncorrected rCBF <40% in multidelay pCASL and Tmax >6 s in DSC-PWI showed moderate consistency (ICC =0.578). Hypoperfusion volume defined by uncorrected CBF <20 mL·100 g^{-1}·min^{-1} in multidelay pCASL and Tmax >6 s in DSC-PWI showed substantial consistency (ICC =0.675). Hypoperfusion volume defined by ATT-corrected CBF <20 mL·100 g^{-1}·min^{-1} in multidelay pCASL and Tmax >6 s in DSC-PWI showed substantial consistency (ICC =0.742).

In the symptomatic chronic group, hypoperfusion volume defined by uncorrected rCBF <40% in multidelay pCASL and Tmax >6 s in DSC-PWI showed weak consistency (ICC =0.292). Hypoperfusion volume defined by uncorrected CBF <20 mL·100 g^{-1}·min^{-1} in multidelay pCASL and Tmax >6 s in DSC-PWI showed moderate consistency (ICC =0.415). Hypoperfusion volume defined by cCBF <20 mL·100 g^{-1}·min^{-1} in multidelay pCASL and Tmax >6 s in DSC-PWI showed substantial consistency (ICC =0.617) (*Table 2*). *Figure 3* shows the representative images of hypoperfusion volume defined by multidelay pCASL and DSC-PWI.

ASL-DWI shows good performance in selecting patients with acute LVOs for EVT

The selection of patients for EVT was determined based

Table 1 Clinical and imaging characteristics of the patients with acute or symptomatic chronic LVOs

Parameters	Total (n=198)	Acute LVOs (n=108)	Symptomatic chronic LVOs (n=90)
Clinical characteristics			
Age (years)	57.0±12.7	58.4±12.2	55.3±13.2
Males	148 (74.7)	84 (77.8)	64 (71.1)
Median baseline NIHSS	6 [1–9]	8 [7–10]	1 [0–2]
Hypertension	125 (63.1)	70 (64.8)	55 (61.1)
Hyperlipidemia	26 (13.1)	16 (14.8)	10 (11.1)
Diabetes mellitus	49 (24.7)	28 (25.9)	21 (23.3)
Atrial fibrillation	16 (8.1)	12 (11.1)	4 (4.4)
Occlusion site			
Intracranial ICA occlusion with or without MCA	99 (50.0)	47 (43.5)	52 (57.8)
Isolated proximal MCA-M1 occlusion	99 (50.0)	61 (56.5)	38 (42.2)
Imaging characteristics			
Infarction core (mL)	1.0 [0–20.5]	16.3 [1.5–38.3]	0 [0–0]
Tmax >6 s (mL)	30.8 [0–92.0]	69.5 [20.0–121.4]	0 [0–36.4]
Uncorrected rCBF <40% (mL)	107.2 [63.5–157.6]	128.8 [76.2–181.1]	78.3 [53.5–129.4]
Uncorrected CBF <20 mL·100 g^{-1}·min^{-1} (mL)	72.5 [25.7–126.3]	84.1 [36.8–133.9]	59.8 [16.6–98.5]
cCBF <20 mL·100 g^{-1}·min^{-1} (mL)	59.7 [23.2–108.6]	74.4 [26.2–118.0]	36.4 [10.1–85.3]

Data are presented as median [IQR], mean ± SD or n (%). LVOs, large vessel occlusions; SD, standard deviation; NIHSS, National Institute of Health Stroke Scale; IQR, interquartile range; ICA, intracranial cerebral artery; MCA-M1, first segment of middle cerebral artery; CBF, cerebral blood flow; rCBF, relative cerebral blood flow; cCBF, corrected cerebral blood flow.

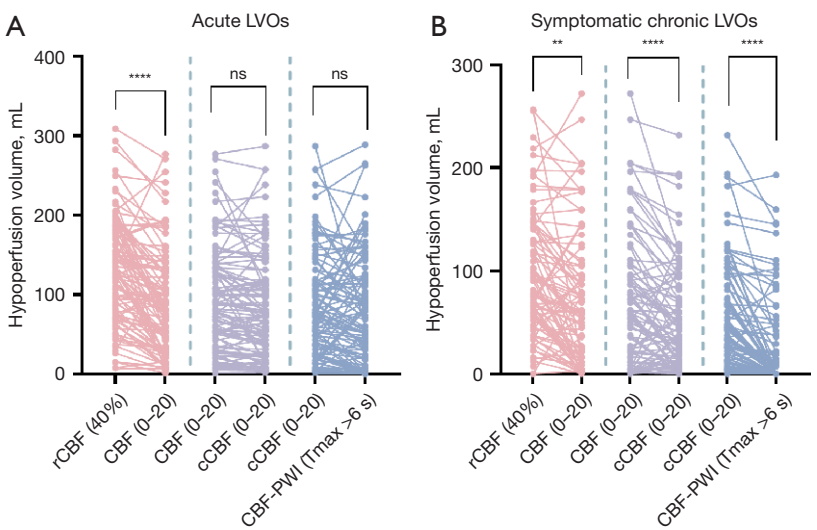

Figure 2 Graphs showing changes in hypoperfusion volume before and after corrected by ATT in acute (A) and symptomatic chronic (B) anterior LVOs. ****, P<0.0001; **, P<0.05. ATT, arterial transit time; DSC-PWI, dynamic susceptibility contrast perfusion weighted imaging; LVOs, large vessel occlusions; CBF, cerebral blood flow; rCBF, relative CBF; cCBF, corrected CBF; ns, not significant.

Table 2 The consistency of hypoperfusion volume in multidelay pCASL and DSC-PWI

Multidelay pCASL	ICC (95% CI)	P value
Acute LVOs		
Hypoperfusion		
Uncorrected rCBF <40%	0.578 (0.170–0.805)	<0.01
Uncorrected CBF <20 mL·100 g^{-1}·min^{-1}	0.675 (0.552–0.768)	<0.01
cCBF <20 mL·100 g^{-1}·min^{-1}	0.742 (0.644–0.816)	<0.01
Symptomatic chronic LVOs		
Uncorrected rCBF <40%	0.292 (−0.094–0.591)	<0.01
Uncorrected CBF <20 mL·100 g^{-1}·min^{-1}	0.415 (0.034–0.653)	<0.01
cCBF <20 mL·100 g^{-1}·min^{-1}	0.617 (0.245–0.793)	<0.01

pCASL, pseudo-continuous arterial spin labeling; DSC-PWI, dynamic-susceptibility-contrast perfusion-weighted-imaging; ICC, intraclass correlation coefficient; CI, confidence interval; LVOs, large vessel occlusions; CBF, cerebral blood flow; rCBF, relative cerebral blood flow; cCBF, corrected cerebral blood flow.

on the DEFUSE 3 trial standard, and the assessment of penumbra and ischemic core were from DSC-PWI as well as ADC. Using selection results based on DSC-PWI as the reference standard, the CBF corrected by ATT showed good performance in selecting patients with acute LVOs for EVT (AUC =0.804, 95% CI: 0.717–0.891) (*Figure 4*). The sensitivity and specificity were 70.9% and 84.9%, respectively.

Discussion

This study compared the consistency between the multidelay pCASL before and after correction by ATT and DSC-PWI in evaluating the hypoperfused tissue volumes in patients with LVOs. The HPT volumes assessed by multidelay pCASL after correction were close to that of DSC-PWI, whether it was acute or symptomatic chronic LVO patients. Moreover, the pCASL based on DEFUSE 3 showed good performance in selecting patients with acute LVOs for thrombectomy. ATT-corrected CBF was closer to the true microcirculation state, for which pCASL mainly detects microvascular perfusion by labeling the hydrogen proton in the blood as a self-contrast tracer (18,19). A number of studies have confirmed that CBF calculated by ASL has a high consistency with the blood perfusion value and glucose metabolism obtained by positron emission tomography (20,21).

The cCBF maps estimated from the multidelay pCASL data and the Tmax maps from the DSC-PWI data showed similar accuracy in identifying patients with acute hypoperfused lesions and the tissue at-risk of infarction for EVT. These findings were in accordance with previously reported findings (22,23). The consensus statement of the International Society for Magnetic Resonance in Medicine (ISMRM) perfusion study group and the European consortium for ASL in dementia-approved specific recommendations for the use of ASL in clinical applications, including the use of the pCASL scheme for scanning and a PLD of 2,000 ms for the adult patients (24). Previous studies have demonstrated that the estimation of the hypoperfusion volume by the long-delay and multidelay pCASL is more accurate compared with the standard-delay ASL (17,25). It is particularly significant to carry out multidelay labeling with prolonged post labeling time, in which patients with LVO have longer ATT than do healthy people.

The pCASL-rCBF <40% threshold relative to the contralateral healthy region was comparable to the PWI-Tmax >6 s and the CTP-Tmax >5.5 s thresholds for the accurate measurement of the penumbra (17,26-28). Wang *et al.* (27) demonstrated that the pCASL perfusion MRI in conjunction with the deep learning algorithm was a promising approach to select patients with AIS for EVT. Yu *et al.* (29) developed an automatic reperfusion scoring system based on the ASPECTS template and demonstrated its clinical utility in selecting patients with AIS for thrombolysis or endovascular treatments. However, we could not guarantee that the contralateral hemisphere is in a normal state of cerebral microcirculation. We found that ATT-corrected ASL is likely to minimize the problem

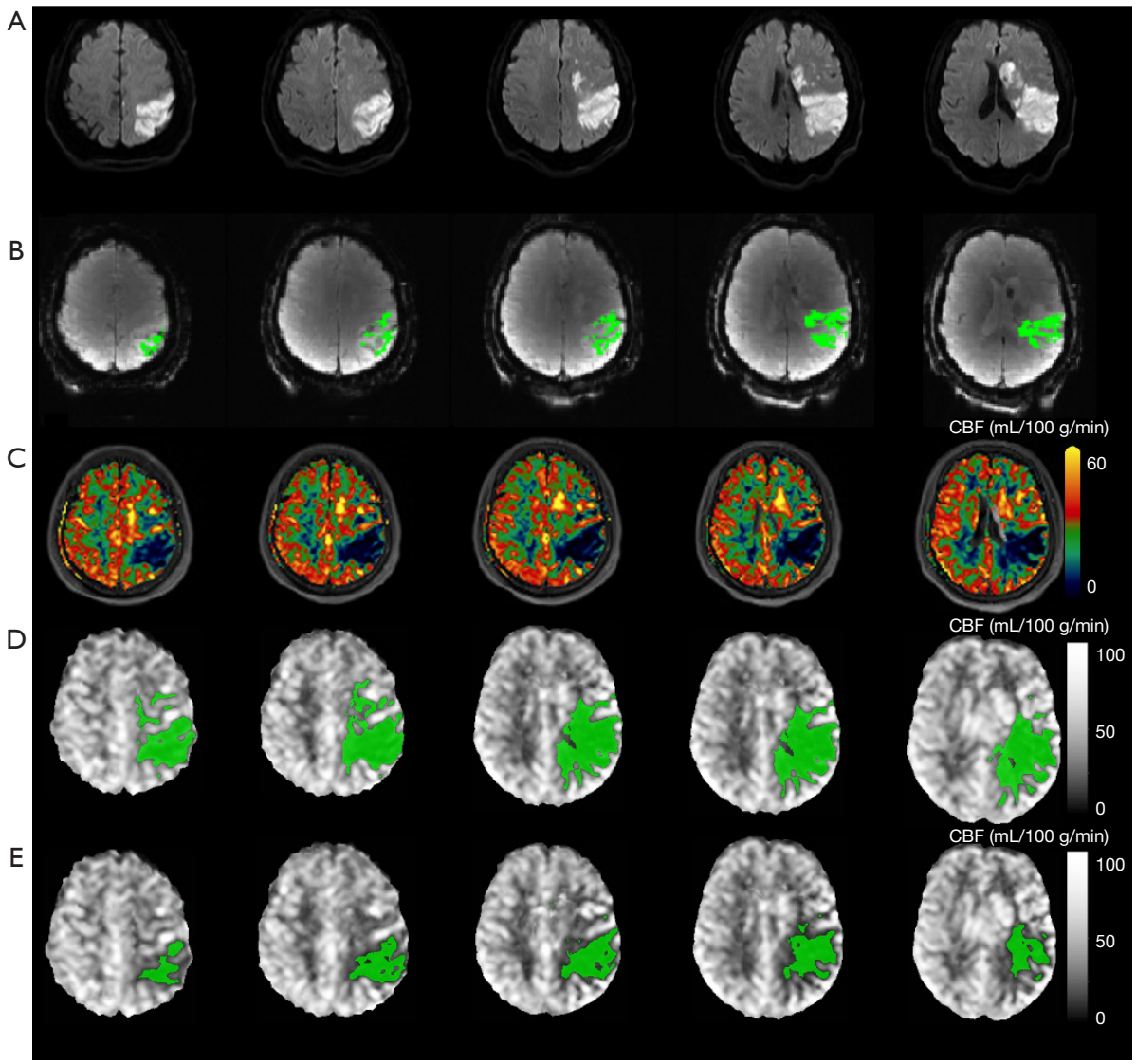

Figure 3 Representative hypoperfusion volume defined by multidelay ASL and DSC-PWI of acute anterior large vessel occlusions. Representative brain MR images of a 76-year-old man with occlusions in the left internal carotid artery. (A) The volume of ischemic core in DWI was 74.1 mL. (B) The hypoperfusion volume defined by time to maximum >6 s (green) was 23.9 mL. (C) CBF corrected by ATT showed hypoperfusion in left parietal and temporal lobe. The hypoperfusion volume was 35.26 mL. (D) The hypoperfusion volume of uncorrected rCBF <40% (green) was 96.84 mL. (E) The hypoperfusion volume of uncorrected CBF <20 mL·100 g^{-1}·min^{-1} (green) was 53.2 mL. ASL, arterial spin labeling; DSC-PWI, dynamic susceptibility contrast perfusion-weighted imaging; MR, magnetic resonance; DWI, diffusion-weighted imaging; CBF, cerebral blood flow; ATT, arterial transit time; rCBF, relative CBF.

of reaching the parenchymal capillary bed and accurately estimate the hypoperfused tissue volumes.

The prognosis of patients with AIS and their quality of life are highly dependent on the choice of treatment. Advanced imaging techniques have been used to quantify the volumes of the infarct core and the penumbra and play an important role in the management of patients with AIS. However, the measurements of the infarct cores based on the DWI and CTP techniques vary significantly and can impact clinical decisions (30,31). DWI and DSC-PWI are the current gold standards for estimating the ischemic core and the penumbra in clinical settings. However, DSC-PWI is performed by injecting the contrast agent, which is contraindicated in patients with renal impairments

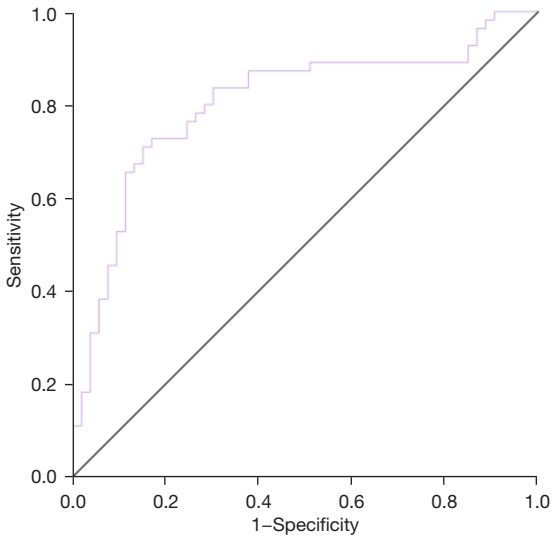

Figure 4 ROC curve analysis of the pCASL corrected by ATT. The ROC curve analysis of the pCASL corrected by ATT based on DEFUSE 3 standard to select patients with AIS for EVT. ROC, receiver operating characteristic; pCASL, pseudo-continuous arterial spin labeling; ATT, arterial transit time; AIS, acute ischemic stroke; EVT, endovascular thrombectomy.

(13,32,33). Furthermore, repeated administration of gadolinium-based contrast agents is linked to MRI signal changes in the deep nuclei of the brain (34). pCASL does not require any contrast and can be performed on all the patients with AIS undergoing MRI, including the elderly, children, and pregnant women. It cannot be performed only for those patients who are contraindicated for MRI. Therefore, the non-invasive ASL perfusion after correction and diffusion MRI can be used routinely for patients with AIS for treatment evaluation as well as post-treatment follow-up of disease progression.

Our study showed good consistency between pCASL and DSC-PWI in estimating the HPT volumes of patients with acute LVOs. Different individuals of LVOs could result in different arriving time of labeled blood flow. Uncorrected ATT resulted in overestimating the volumes of HPT. Fan *et al.* (35) reported that long-label long-delay ASL acquisitions (PLD =4.0 s) were necessary to accurately estimate cortical CBF in patients with moyamoya disease. Consistent with the previous studies (36,37), CBF maps of patients with acute LVOs based on the multi-delay and long delay pCASL were more accurate. This suggested that patients with LVOs require longer PLDs to accurately estimate HPT volumes. Multiple PLDs cover a wider range of time, avoiding the underestimation of CBF caused by too short PLD time. Therefore, our data suggest that accurate estimation of hypoperfused tissue volumes in patients with acute LVOs requires correction by ATT. In such cases, a mixture of high and low ASL signal intensity, referred to as the arterial transit artifacts (ATAs), was observed because the PLD was not long enough for the labeled blood to reach the parenchymal capillary bed (38). The presence of ATA affects the accuracy of estimating hypoperfused volumes. There was good agreement between the 2 imaging methods in assessing the hypoperfused volume, but the multi-delay pCASL exaggerated the hypoperfused volume because of ATA (Figure S1). De Havenon *et al.* (39) suggested that ATA on ASL were indicative of improved neurologic outcomes in patients with ischemic stroke at hospital discharge. However, this did not correlate with the findings in our study. Therefore, using the ATT-corrected CBF technique minimizes the problem of reaching the parenchymal capillary bed and accurately estimates the hypoperfused tissue volumes. Future studies can improve the consistency between the pCASL and DSC-PWI by correcting CBF and increasing the number of PLDs in patients with symptomatic, chronic LVOs.

Our study has several limitations. Firstly, the MRI data analysis and automated volume calculation was performed on a cohort of patients from a single center; this could lead to sampling bias. We also evaluated pCASL and DSC-PWI data for all the participants and did not perform any manual corrections during the segmentation process. Secondly, the volume of hypoperfused lesions was estimated and analyzed for 108 patients with acute LVOs and 90 patients with symptomatic chronic LVOs. In the future, larger cohorts from multiple centers need to be analyzed to improve the accuracy of pCASL and validate our findings. Thirdly, we did not perform ASL examinations of the participants after mechanical thrombectomy within 24 hours. We also did not correlate our findings with the clinical outcomes of the patients or estimate the final stroke volume in the follow-up imaging. These aspects were outside the focus of our study. The primary goal of this investigation was to evaluate the technical differences or similarities between the 2 perfusion methods in stroke diagnostics. In the future, large-scale multi-center clinical studies are required to evaluate the efficacy of pCASL in accurately estimating hypoperfused tissue volumes and hemorrhagic transformation in patients with AIS and predict the follow-up infarction in patients with AIS who have not undergone reperfusion therapy.

Conclusions

The volume of hypoperfusion defined by corrected CBF <20 mL·100 g^{-1}·min^{-1} is close to that of DSC-PWI in acute and chronic symptomatic LVOs patients. Multidelay pCASL adjusted by ATT is more accurate in identifying microcirculation dysfunction.

Acknowledgments

The authors thank all the participants in the study for their contributions and all the neurologists and medical radiation technologists in Tianjin First Central Hospital for their support.

Footnote

Reporting Checklist: The authors have completed the STROBE reporting checklist. Available at https://qims.amegroups.com/article/view/10.21037/qims-24-1560/rc

Funding: This study was supported by the National Natural Science Foundation of China (Nos. 82171916 and 81871342), the Natural Science Foundation of Tianjin (Nos. 21CYBJC01580 and 22JCYBJC01270), Tianjin Health Science and Technology Project (specific projects of key disciplines) (No. TJWJ2022XK019), and Tianjin Key Medical Discipline (Specialty) Construction Project (No. TJYXZDXK-041A).

Conflicts of Interest: All authors have completed the ICMJE uniform disclosure form (available at https://qims.amegroups.com/article/view/10.21037/qims-24-1560/coif). J.Z. is a current employee of Siemens Healthineers. The other authors have no conflicts of interest to declare.

Ethical Statement: The authors are accountable for all aspects of the work in ensuring that questions related to the accuracy or integrity of any part of the work are appropriately investigated and resolved. This retrospective study was conducted in accordance with the Declaration of Helsinki (as revised in 2013). The study was approved by institutional ethics board of Tianjin First Central Hospital (No. 2017N002KY) and the requirement of individual consent for this retrospective analysis was waived.

References

1. Ma Q, Li R, Wang L, Yin P, Wang Y, Yan C, Ren Y, Qian Z, Vaughn MG, McMillin SE, Hay SI, Naghavi M, Cai M, Wang C, Zhang Z, Zhou M, Lin H, Yang Y. Temporal trend and attributable risk factors of stroke burden in China, 1990-2019: an analysis for the Global Burden of Disease Study 2019. Lancet Public Health 2021;6:e897-906.
2. Guo X, Miao Z. Advances in mechanical thrombectomy for acute ischaemic stroke from large vessel occlusions. Stroke Vasc Neurol 2021;6:649-57.
3. Albers GW, Marks MP, Kemp S, Christensen S, Tsai JP, Ortega-Gutierrez S, et al. Thrombectomy for Stroke at 6 to 16 Hours with Selection by Perfusion Imaging. N Engl J Med 2018;378:708-18.
4. Nogueira RG, Jadhav AP, Haussen DC, Bonafe A, Budzik RF, Bhuva P, et al. Thrombectomy 6 to 24 Hours after Stroke with a Mismatch between Deficit and Infarct. N Engl J Med 2018;378:11-21.
5. Campbell BCV, De Silva DA, Macleod MR, Coutts SB, Schwamm LH, Davis SM, Donnan GA. Ischaemic stroke. Nat Rev Dis Primers 2019;5:70.
6. Seners P, Yuen N, Mlynash M, Snyder SJ, Heit JJ, Lansberg MG, Christensen S, Albucher JF, Cognard C, Sibon I, Obadia M, Savatovsky J, Baron JC, Olivot JM, Albers GW; Mismatch Prevalence Investigators. Quantification of Penumbral Volume in Association With Time From Stroke Onset in Acute Ischemic Stroke With Large Vessel Occlusion. JAMA Neurol 2023;80:523-8.
7. Derdeyn CP. Hemodynamics and oxygen extraction in chronic large artery steno-occlusive disease: Clinical applications for predicting stroke risk. J Cereb Blood Flow Metab 2018;38:1584-97.
8. Li J, Chen XY, Soo Y, Leung TW, Zeng J, Wong KS. Benign Oligemia in Subacute Stage Is Associated with Borderzone Infarction in Stroke Patients Caused by Intracranial Large Artery Disease. Eur Neurol 2017;77:80-6.
9. Huang D, Guo Y, Guan X, Pan L, Zhu Z, Chen Z, Dijkhuizen RM, Duering M, Yu F, Boltze J, Li P. Recent

advances in arterial spin labeling perfusion MRI in patients with vascular cognitive impairment. J Cereb Blood Flow Metab 2023;43:173-84.
10. Wang X, Bishop C, O'Callaghan J, Gayhoor A, Albani J, Theriault W, Chappell M, Golay X, Wang D, Becerra L. MRI assessment of cerebral perfusion in clinical trials. Drug Discov Today 2023;28:103506.
11. Yan C, Yu F, Zhang Y, Zhang M, Li J, Wang Z, Lu J, Ma Q. Multidelay Arterial Spin Labeling Versus Computed Tomography Perfusion in Penumbra Volume of Acute Ischemic Stroke. Stroke 2023;54:1037-45.
12. Woolen SA, Shankar PR, Gagnier JJ, MacEachern MP, Singer L, Davenport MS. Risk of Nephrogenic Systemic Fibrosis in Patients With Stage 4 or 5 Chronic Kidney Disease Receiving a Group II Gadolinium-Based Contrast Agent: A Systematic Review and Meta-analysis. JAMA Intern Med 2020;180:223-30.
13. Cha MJ, Kang DY, Lee W, Yoon SH, Choi YH, Byun JS, Lee J, Kim YH, Choo KS, Cho BS, Jeon KN, Jung JW, Kang HR. Hypersensitivity Reactions to Iodinated Contrast Media: A Multicenter Study of 196 081 Patients. Radiology 2019;293:117-24.
14. Barnett HJ, Taylor DW, Eliasziw M, Fox AJ, Ferguson GG, Haynes RB, Rankin RN, Clagett GP, Hachinski VC, Sackett DL, Thorpe KE, Meldrum HE, Spence JD. Benefit of carotid endarterectomy in patients with symptomatic moderate or severe stenosis. North American Symptomatic Carotid Endarterectomy Trial Collaborators. N Engl J Med 1998;339:1415-25.
15. Myrcha P, Gloviczki P. A systematic review of endovascular treatment for chronic total occlusion of the internal carotid artery. Ann Transl Med 2021;9:1203.
16. van der Thiel M, Rodriguez C, Giannakopoulos P, Burke MX, Lebel RM, Gninenko N, Van De Ville D, Haller S. Brain Perfusion Measurements Using Multidelay Arterial Spin-Labeling Are Systematically Biased by the Number of Delays. AJNR Am J Neuroradiol 2018;39:1432-8.
17. Bivard A, Krishnamurthy V, Stanwell P, Levi C, Spratt NJ, Davis S, Parsons M. Arterial spin labeling versus bolus-tracking perfusion in hyperacute stroke. Stroke 2014;45:127-33.
18. Lin T, Qu J, Zuo Z, Fan X, You H, Feng F. Test-retest reliability and reproducibility of long-label pseudo-continuous arterial spin labeling. Magn Reson Imaging 2020;73:111-7.
19. Zhao MY, Václavů L, Petersen ET, Biemond BJ, Sokolska MJ, Suzuki Y, Thomas DL, Nederveen AJ, Chappell MA. Quantification of cerebral perfusion and cerebrovascular reserve using Turbo-QUASAR arterial spin labeling MRI. Magn Reson Med 2020;83:731-48.
20. Rischka L, Godbersen GM, Pichler V, Michenthaler P, Klug S, Klöbl M, Ritter V, Wadsak W, Hacker M, Kasper S, Lanzenberger R, Hahn A. Reliability of task-specific neuronal activation assessed with functional PET, ASL and BOLD imaging. J Cereb Blood Flow Metab 2021;41:2986-99.
21. Wang J, Sun H, Cui B, Yang H, Shan Y, Dong C, Zang Y, Lu J. The Relationship Among Glucose Metabolism, Cerebral Blood Flow, and Functional Activity: a Hybrid PET/fMRI Study. Mol Neurobiol 2021;58:2862-73.
22. Wang DJ, Alger JR, Qiao JX, Gunther M, Pope WB, Saver JL, Salamon N, Liebeskind DS; UCLA Stroke Investigators. Multi-delay multi-parametric arterial spin-labeled perfusion MRI in acute ischemic stroke - Comparison with dynamic susceptibility contrast enhanced perfusion imaging. Neuroimage Clin 2013;3:1-7.
23. Wang DJ, Alger JR, Qiao JX, Hao Q, Hou S, Fiaz R, Gunther M, Pope WB, Saver JL, Salamon N, Liebeskind DS; UCLA Stroke Investigators. The value of arterial spin-labeled perfusion imaging in acute ischemic stroke: comparison with dynamic susceptibility contrast-enhanced MRI. Stroke 2012;43:1018-24.
24. Alsop DC, Detre JA, Golay X, Günther M, Hendrikse J, Hernandez-Garcia L, Lu H, MacIntosh BJ, Parkes LM, Smits M, van Osch MJ, Wang DJ, Wong EC, Zaharchuk G. Recommended implementation of arterial spin-labeled perfusion MRI for clinical applications: A consensus of the ISMRM perfusion study group and the European consortium for ASL in dementia. Magn Reson Med 2015;73:102-16.
25. Yu H, Ouyang Y, Feng Y, Sun S, Zhang L, Liu Z, Tian H, Xie S. Comparison of single-postlabeling delay and seven-delay three-dimensional pseudo-continuous arterial spin labeling in the assessment of intracranial atherosclerotic disease. Quant Imaging Med Surg 2023;13:2514-25.
26. Zaharchuk G. Arterial spin-labeled perfusion imaging in acute ischemic stroke. Stroke 2014;45:1202-7.
27. Wang K, Shou Q, Ma SJ, Liebeskind D, Qiao XJ, Saver J, Salamon N, Kim H, Yu Y, Xie Y, Zaharchuk G, Scalzo F, Wang DJJ. Deep Learning Detection of Penumbral Tissue on Arterial Spin Labeling in Stroke. Stroke 2020;51:489-97.
28. Ter Schiphorst A, Charron S, Hassen WB, Provost C, Naggara O, Benzakoun J, Seners P, Turc G, Baron JC, Oppenheim C. Tissue no-reflow despite full recanalization following thrombectomy for anterior circulation stroke

with proximal occlusion: A clinical study. J Cereb Blood Flow Metab 2021;41:253-66.
29. Yu S, Ma SJ, Liebeskind DS, Yu D, Li N, Qiao XJ, Shao X, Yan L, Yoo B, Scalzo F, Hinman JD, Sharma LK, Rao N, Jahan R, Tateshima S, Duckwiler GR, Saver JL, Salamon N, Wang DJ. ASPECTS-based reperfusion status on arterial spin labeling is associated with clinical outcome in acute ischemic stroke patients. J Cereb Blood Flow Metab 2018;38:382-92.
30. Copen WA, Morais LT, Wu O, Schwamm LH, Schaefer PW, González RG, Yoo AJ. In Acute Stroke, Can CT Perfusion-Derived Cerebral Blood Volume Maps Substitute for Diffusion-Weighted Imaging in Identifying the Ischemic Core? PLoS One 2015;10:e0133566.
31. Copen WA, Yoo AJ, Rost NS, Morais LT, Schaefer PW, González RG, Wu O. In patients with suspected acute stroke, CT perfusion-based cerebral blood flow maps cannot substitute for DWI in measuring the ischemic core. PLoS One 2017;12:e0188891.
32. Mathur M, Jones JR, Weinreb JC. Gadolinium Deposition and Nephrogenic Systemic Fibrosis: A Radiologist's Primer. Radiographics 2020;40:153-62.
33. Pasquini L, Napolitano A, Visconti E, Longo D, Romano A, Tomà P, Rossi Espagnet MC. Gadolinium-Based Contrast Agent-Related Toxicities. CNS Drugs 2018;32:229-40.
34. Gulani V, Calamante F, Shellock FG, Kanal E, Reeder SB; International Society for Magnetic Resonance in Medicine. Gadolinium deposition in the brain: summary of evidence and recommendations. Lancet Neurol 2017;16:564-70.
35. Fan AP, Guo J, Khalighi MM, Gulaka PK, Shen B, Park JH, Gandhi H, Holley D, Rutledge O, Singh P, Haywood T, Steinberg GK, Chin FT, Zaharchuk G. Long-Delay Arterial Spin Labeling Provides More Accurate Cerebral Blood Flow Measurements in Moyamoya Patients: A Simultaneous Positron Emission Tomography/MRI Study. Stroke 2017;48:2441-9.
36. Shirzadi Z, Stefanovic B, Chappell MA, Ramirez J, Schwindt G, Masellis M, Black SE, MacIntosh BJ. Enhancement of automated blood flow estimates (ENABLE) from arterial spin-labeled MRI. J Magn Reson Imaging 2018;47:647-55.
37. Ishida S, Kimura H, Isozaki M, Takei N, Fujiwara Y, Kanamoto M, Kosaka N, Matsuda T, Kidoya E. Robust arterial transit time and cerebral blood flow estimation using combined acquisition of Hadamard-encoded multi-delay and long-labeled long-delay pseudo-continuous arterial spin labeling: a simulation and in vivo study. NMR Biomed 2020;33:e4319.
38. Zaharchuk G. Arterial Transit Awesomeness. Radiology 2020;297:661-2.
39. de Havenon A, Haynor DR, Tirschwell DL, Majersik JJ, Smith G, Cohen W, Andre JB. Association of Collateral Blood Vessels Detected by Arterial Spin Labeling Magnetic Resonance Imaging With Neurological Outcome After Ischemic Stroke. JAMA Neurol 2017;74:453-8.

Cite this article as: Zhao C, Cao C, Ren L, Wang H, Wu G, Fu D, Zhu J, Chai C, Guo Y, Xia S. Estimation of hypoperfused tissue volume in large vessel occlusions: pseudo-continuous arterial spin labeling versus dynamic susceptibility contrast perfusion-weighted imaging. Quant Imaging Med Surg 2025;15(3):2053-2064. doi: 10.21037/qims-24-1560

